AGU ADVANCING EARTH AND SPACE SCIENCE

Geophysical Research Letters

RESEARCH LETTER
10.1029/2020GL092137

Biological Cohesion as the Architect of Bed Movement Under Wave Action

Xindi Chen[1,2], Changkuan Zhang[2], Ian H. Townend[3], David M. Paterson[4], Zheng Gong[2], Qin Jiang[2], Qian Feng[5], and Xiping Yu[1]

[1]State Key Laboratory of Hydroscience and Engineering, Department of Hydraulic Engineering, Tsinghua University, Beijing, China, [2]College of Harbor, Coastal and Offshore Engineering, Hohai University, Nanjing, China, [3]School of Ocean and Earth Science, National Oceanography Centre, University of Southampton, Southampton, UK, [4]Sediment Ecology Research Group, Scottish Oceans Institute, School of Biology, University of St Andrews, St Andrews, UK, [5]College of Environment, Hohai University, Nanjing, China

Key Points:

- Cohesive extracellular polymeric substances largely affect the bed mobility under wave action showing a destabilization of the system
- Small amounts of substrate biological cohesion act to liquefy an otherwise stable bed and increase erosion up to three times
- A framework is proposed showing how biological cohesion can put coastal sediment at risk by increasing its vulnerability to waves

Supporting Information:

- Supporting Information S1

Correspondence to:
X. Yu,
yuxiping@tsinghua.edu.cn

Citation:
Chen, X., Zhang, C., Townend, I. H., Paterson, D. M., Gong, Z., Jiang, Q., et al. (2021). Biological cohesion as the architect of bed movement under wave action. *Geophysical Research Letters*, *48*, e2020GL092137. https://doi.org/10.1029/2020GL092137

Received 15 DEC 2020
Accepted 7 JAN 2021

Abstract Cohesive extracellular polymeric substances (EPS) generated by microorganisms abundant on Earth are regarded as bed "stabilizers" increasing the erosion threshold in sedimentary systems. However, most observations of this phenomenon have been taken under steady flow conditions. In contrast, we present how EPS affect the bed movement under wave action, showing a destabilization of the system. We demonstrate a complex behavior of the biosedimentary deposits, which encompasses liquefaction, mass motion, varying bed formations and erosion, depending on the amount of EPS present. Small quantities of EPS induce higher mobility of the sediments, liquefying an otherwise stable bed. Bed with larger quantities of EPS undergoes a synchronized mechanical oscillation. Our analysis clarifies how biological cohesion can potentially put coastal wetlands at risk by increasing their vulnerability to waves. These findings lead to a revised understanding of the different roles played by microbial life, and their importance as mediators of seabed mobility.

Plain Language Summary The term "ecosystem engineering" emerged in the 1990s, which commonly refers to the activities of larger organisms like mangroves. However, while people think that bigger organisms generate bigger potential engineering effects, there may be microscale organisms who can result in significant impacts on the ecosystems through their number rather than their size. Currently, cohesive extracellular polymeric substances (EPS) generated by microorganisms have been widely reported to increase the threshold for sediment erosion by flowing water, which is known as "biostabilization." However, we demonstrate that this is not the case under wave action. On the contrary, EPS show a destabilization effect of the system, turning an otherwise stable sedimentary bed into "soup." Our analysis clarifies how neglecting even low content of EPS can result in inaccurate prediction of the bed stability and coastal safety under wave action. The risk of bed liquefaction is expected to pose potential threats to wetlands where microbial communities occupy habitats while the production of EPS is much higher. The misinterpretation of the vulnerability of wetlands when exposed to waves could put the existing ecosystems at risk, considering that these ecosystem services are valued at about US$10,000 per hectare.

1. Introduction

Microbial life and their secreted extracellular polymeric substances (EPS) serve as cooperative "ecosystem engineers," which strongly influence sediment texture in both the earliest and modern sedimentary environments (Davis et al., 2006; Marani et al., 2007; Mariotti et al., 2014; Noffke et al., 2006). In fact, the stabilizing effect of EPS matrix in surficial biofilms has been widely reported over the last 20 years, and is known as "biostabilization" inhabiting depositional systems (Chen et al., 2017a; Gerbersdorf & Wieprecht, 2015; Packman, 2013; Paterson et al., 2018; Taylor & Paterson, 1998). Despite growing research interest, uncertainties and debates remain on some fundamental issues, such as the various behavior under different hydrodynamic systems and scales (Tolhurst et al., 2002). For instance, the studies which support the stabilizing effect rely almost completely on aquatic environments with steady flow conditions, where surficial erosion and bedforms are the primary concerns (~cm in upper layers) (Le Hir et al., 2007; Parsons et al., 2016; Van Colen et al., 2014; Vignaga et al., 2013). In the marine environment, however, wave action may induce liquefaction, where a certain depth of a sedimentary bed, ranging from tens of centimeters

to meters below the bed surface, turns into a liquid state (Sumer et al., 2006). This can cause a powerful sediment flushing that moves downslope and across the shelf offshore (Craig et al., 2020; Mcanally et al., 2007; Mountjoy et al., 2018). Bed liquefaction describes quite a different process from surficial erosion, and is the cause of many catastrophic coastal disasters globally (Chung et al., 2006; Franco, 1994; Travis, 2005). What is less clear is whether microbiology acts as a stabilizer of the bed, helping to limit the potential for liquefaction, or not.

The literature on liquefaction in engineering is extensive, spanning more than 50 years (Lewis & Partridge, 1967; Nichols et al., 1994; Sumer, 2009). However, microbiological effects have not been widely recognized in liquefaction-related studies, despite the fact that the upper oceanic sediment, down to 50 cm depth, holds the majority of bacteria and archaea existing on Earth (5×10^{28} cells; Danovaro et al., 2015; Flemming & Wuertz, 2019). A liquefaction zone was reported at a wetland restoration site, with abundant microalgae as primary productors supporting fish habitats, which caused severe damage to the ecosystem (Iwakuni, Japan, September 2016). The liquefaction had not been predicted based on experimental data using grains that were free from biological material. It seems that biological activities could possibly affect the risk of liquefaction, however the mechanism remains unknown. The unusually limited attention paid to biological cohesion and its effect in wave induced liquefaction probably reflects the multidisciplinary nature of the problem, but the role of EPS in geo-engineering systems is now being more widely recognized (Craig et al., 2020).

Experiments were conducted in a wave flume to examine the behavior of the bed as the EPS content in a well-sorted fine sand was progressively increased. Liquefaction was judged from the temporal variation of pore pressure, and linked to the deformation of the sediment-water interface determined using time-lapse photography. Sediment erosion and suspension was measured using an optical back-scatter turbidity sensor. This study provides the first systematic experiments to explore the effect of the pervasive 'background' EPS on the susceptibility of sandy bed to liquefaction, in contrast to the previous investigations that focused on the "biostabilization" of surficially accumulated EPS under steady flow conditions.

2. Materials and Methods

2.1. Experimental Setup

The present work describes laboratory experiments conducted in a 80 m-long, 0.5 m-wide, and 1.5 m-high laboratory wave flume, where a pit filled with a 0.25 m-thick sediment bed was created to examine the influence of pervasive biological cohesion on bed susceptibility to wave-induced liquefaction (see Figure S1a for information about the flume). The sediment bed was composed of a mixture of well-sorted fine sand (D_{50} = 0.165 mm, see Figure S2 for the grain size distribution) and EPS with different quantities (0%–0.1% by weight, Table 1). Pore-water pressure and water surface elevation were measured by pressure sensors and wave gauges, respectively (Figure S1b). Xanthan gum, which is a bacterial polymer, shares chemical similarities with a wide variety of naturally occurring EPS, and is widely used as a substitute for EPS in marine ecology, soil science, and sediment stability research (Craig et al., 2020; Garcı A-Ochoa et al., 2000; Van Colen et al., 2014; X. Zhang et al., 1996). Pretest bed samples were taken to determine the fraction of EPS (Table 1). The EPS extraction and measurements were based on the polysaccharide content. A sinusoidal input wave with a wave height of 0.12 m and period of 1.6 s was used for all test runs, in a water depth of 0.35 m. Video cameras were used to record the bed response, in addition to the pore-water pressure and water surface elevation measurements. Liquefaction was judged from the temporal variation of pore pressure, and linked to the deformation of the sediment-water interface determined using time-lapse photography. Sediment erosion and suspension was measured using an optical backscatter sensor (OBS 3+).

2.2. Preparation of the Bed

The sedimentary bed mixes are listed in Table 1 and range from 0% to 0.1% EPS (xanthan, see supporting information Text S1 for the EPS analysis). Sand-EPS mixtures used for experiments were made in the laboratory, by mixing natural dry sand and commercial xanthan with the determined content ratios. The xanthan (in a dry powder form) was first dissolved by agitation in water (one-part freshwater to four-parts sand/xanthan) for l0∼20 min, after which any foam was removed from the surface of the solution. The liquid

Table 1
Parameters for the Sand-EPS Experiments

Test*	EPS (%)	Test duration (s)	Liquefaction (-)	T_{bs}/T_{bb} (s/s)	T_{es}/T_{eb} (s/s)	Final bed state (-)	Max SSC (g L^{-1})	Average SSC (g L^{-1})
1	0	1,580	No	—	—	R	6.51	3.59
2	0.005	1,500	Yes	23/58	1,303/523	R	7.94	2.17
3	0.01	1800	Yes	11/23	1,772/469	R	10.61	2.58
4	0.02	1,550	Yes	13/28	—	F	19.17	7.03
5	0.05	1,470	Yes	9/38	—	F	3.19	1.71
6	0.1	1,550	Oscillation	0/0	—	F	3.17	1.08

EPS, extracellular polymeric substances, represented by xanthan gum proxy. T is time and subscripts "bs" and "bb" refer to the bed surface and bed bottom, respectively. T_{bs}/T_{bb} is the ratio of the time to liquefaction in the two layers, reflecting how liquefaction first appears at the surface and progressively extends to the bed. Similarly, subscripts "es" and "eb" refer to the end of liquefaction at the surface and bed, respectively. The former is defined by the appearance of a rippled bed and the latter by the initiation of pore pressure dissipation at the bed bottom. The ratio T_{es}/T_{eb} indicates how the liquefaction gradually ends for bottom to top. In this study, only in the low EPS cases (Test 2 and 3), liquefaction stopped before the end of the test and ripples appeared. However, it should be noted that pore pressure dissipation can be reached for all liquefaction cases if time permitted. Final bed state is the state of the bed surface at the end of the test where F is a flat bottom and R is a rippled bed. SSC is the suspended sediment concentration measured using the optical backscatter sensor (OBS). All tests were run in a water depth = 0.35 m with a wave height = 0.12 m and wave period = 1.6 s.

xanthan was then added into the dry sand and stirred to form a uniform mixture. This resulted in a slurry, which was spread evenly, filling the pit to make a flat bed with a depth of 25 cm and length of 1 m (Figure S1b). The flume was then gradually filled with the required amount of freshwater (water depth of 0.45 m) and left for 20–22 h before the test was conducted. Here, note that since cohesion is enhanced by saline conditions, the effect may be greater in marine systems (Spears et al., 2008). Also note that the "abiotic" case is simply without added xanthan. It would be different if the situation without biofilms (which would require sterilization) would be compared to the one with biofilms.

2.3. Instrumentation

Three wave gauges (Yu Fan Technology Co, Chengdu) for recording water elevation were placed at the upstream edge of the pit to measure the incident wave height, the downstream edge to measure the wave height after passing the bed, and above the pore pressure sensors. The pressure transducers (HC-25, Rui-Heng Chang Tai Technology Co, Beijing) for measuring pore-water pressure were installed in the middle of the pit at three different depths (Figure S1b), $z = 0.01$, 0.09 and 0.23 m, where z was the vertical distance below the bed surface. An OBS 3+ (Campbell Scientific, Inc.) located 0.2 m downstream from the front edge of the pit and 0.035 m above the bed surface was used to measure the real-time suspended sediment concentration (the calibration of the OBS for the sand grains used in this study can be found in Figure S3). The monitoring range depends on sediment size, particle shape, and reflectivity. For the sediment used in this study, the maximum concentration was below 20 kg/m^3, which was within the linear region of the OBS sensor (Figure S3). Pore-water pressure, water elevation and suspended sediment concentration (SSC) were measured simultaneously.

2.4. Time Development of EPP

The period-averaged excess-pore pressure, $\overline{p}$ is calculated as:

$$\overline{p} = \frac{1}{T}\int_{t}^{t+T} p\,dt$$

where p is the excess-pore pressure at time t and T is the period for calculation. The value of the initial mean normal effective stress, σ_0 defined by:

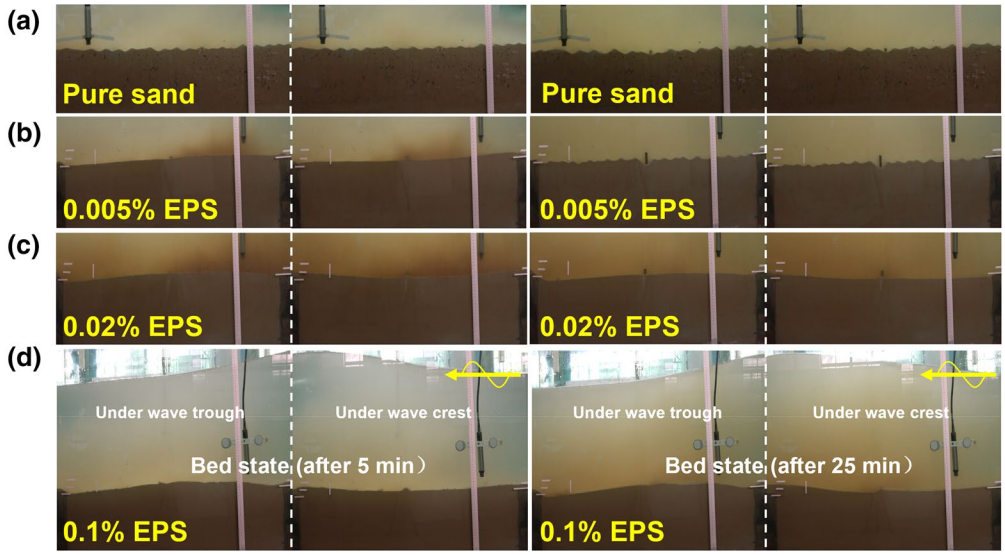

Figure 1. Photographs of bed state during tests. (a) Test 1 (0% EPS), (b) Test 2 (0.005%), (c) Test 4 (0.02%), and (d) Test 6 (0.1%), looking in the side view of the flume and perpendicular to the direction of wave progression. Two bed states under a wave trough are given after 5 min (left column) and 25 min of wave action (right column). The length of the pit is 1 m. EPS, extracellular polymeric substances.

$$\sigma_0 = \gamma' z \frac{1 + 2k_0}{3}$$

with, z is the depth from the bed surface/water-bed interface shown in Figure S1b. k_0 is the coefficient of lateral earth pressure at rest and the value is determined from Jaky's equation, $k_0 = 1 - \sin\varphi$, where φ is the friction angle (Lambe & Whitman, 1969). In this study, φ of all sediment samples were measured by triaxial shear test, giving a mean value of 31°, which equates to a k_0 of 0.48.$\gamma'$was the submerged specific weigh of the sediment,

$$\gamma' = \gamma_{sat} - \gamma$$

where γ_{sat} is the specific weight of the soil, and γ_{sat} = 19.8, 19.6, 19.0, 18.6, 18.3, 18.1 N/m^3, for 0%, 0.005%, 0.01%, 0.02%, 0.05%, 0.1% EPS, respectively, and the value for γ is 9.8. Therefore,σ_0 for z = 0.23 is 1.50, 1.47, 1.40, 1.33, 1.27, 1.25, for each EPS content, correspondingly. The bed is liquefied when $\overline{p}$ exceeds σ_0, and this criterion for the onset of liquefaction has been discussed in greater detail (Sumer et al., 2012).

3. Results and Discussion

3.1. Abiotic Case

In the abiotic case, sediment moved as either bedload or as suspended load. Ripples developed and migrated (Figure 1a) while SSC increased to an averaged value of ~3.6 kg/m^3 (Figure S4). Pore pressure rapidly increased to ~0.1 Pa at the onset of wave load, and then dissipated and oscillated around zero (Figure S4). The susceptibility to liquefaction of the sandy bed under this set of wave condition was low. The result is in good agreement with other clean sand results, which involved sand with a similar grain diameter (Tzang & Ou, 2006).

3.2. Effect of EPS on Bed Mobility

The bed mobility increases and the bedform varies as the EPS increases from 0% to 0.1% (Figure 1). The upper range of 0.1% reflects the limit for a solid-liquid transition to occur (T_{bs}/T_{bb} column in Table 1). According to previous studies, higher critical shear stress is required to move sediment under currents when EPS

is present and this is considered as evidence of the bed stabilizing effect of EPS (Chen et al., 2017a, 2017b; Gerbersdorf & Wieprecht, 2015; Packman, 2013). However, results in the present study show that even at a comparatively low level of EPS (0.005%), liquefaction took place under the action of waves, that is, the bed was destabilized. In the low EPS cases, liquefaction stopped before the end of the test and ripples appeared (Figure 1b, T_{es}/T_{eb} in Table 1). Hence, the bedforms (Figure 1b) were similar to the abiotic case (Figure 1a), albeit with different final dimension based on the final bed geometry. Critically, by considering only the final bedforms, the history of bed deformation and period of liquefaction was overlooked. Moreover, an increase of the EPS shortened the time at which the cycle of mass motion first appeared (T_{bs} in Table 1) and also the development time of liquefaction throughout the depth profile (T_{bb} in Table 1).

A liquefaction phase was again observed with a slightly higher concentration of EPS (Test 4 with 0.02% EPS), but the bed surface was flat after the waves stopped (Table 1), rather than rippled, and there was only a limited amount of mass motion in the last few minutes (Figure 1c).

In the 0.1% EPS case, the bed oscillated from the beginning of the test (Table 1). The bed surface rose as a wave trough passed and lowered under the wave crests. The undulation showed an almost invariant amplitude during the test. The bed acted as an elastic membrane under waves and there was no solid-liquid transition phase observed. This is quite different from the results observed in other cases with lower amounts of EPS present, where no sediment motion was observed until the onset of liquefaction (T_{bs} in Table 1). This phenomenon echoes the early study recording a similar "oscillatory effect" from a local patch of biofilms observed in the field, where the surface reacted like the skin of a drum, vibrating slightly (Paterson, 1989). Nevertheless, the biological effect was far stronger than physical cohesion alone, where sand becomes prone to liquefaction for clay contents of up to 10%, beyond which the mixture is stabilized and no longer susceptible to liquefaction (Gratchev et al., 2006).

3.3. The Temporal Variation of EPP

The time variation of the excess-pore pressure (EPP) at the measured position, that is, pore water pressure in excess of the hydrostatic condition, is an established indicator for local liquefaction, used to explain the process in further detail (Gratchev et al., 2006; Sumer et al., 2006). Whilst the EPP inside the bed oscillated in phase with the waves (Figure 2a), the period-averaged EPP ($\overline{p}$ dash lines in Figure 2a, see 2.4 for the calculation) built up in all the biological cases. After several cycles, $\overline{p}$ reached a form of dynamic "equilibrium," $\overline{p}_{max}$. When $\overline{p}_{max}$ exceeded the initial mean normal effective stress σ_0 (see Section 2.4 for the evaluation), the particles were then suspended and moved with the oscillatory motion generated by the waves. This has been commonly used to designate the onset of seabed liquefaction (Sumer et al., 2012). The behavior of the bed with an EPS range of 0.005%–0.02% in this study is in good agreement with this criterion (Figure 2a).

With further increases in EPS however, the value of $\overline{p}_{max}$ no longer exceeded σ_0 Liquefaction occurred with larger, but still small quantities of EPS, even though $\overline{p}_{max}$ was much lower than the threshold value of σ_0 (0.05% EPS, Figure 2a). When mixed with an even higher level of EPS (i.e., 0.1%), there was no accumulation but a drop of EPP, followed by a constant but negative value of period-averaged EPP (Figure 2a).

After an initial build-up of pore pressure, the beds with lower EPS content (in Test 2 and 3) lost stability. They transitioned through a liquefaction phase, before the onset of consolidation and the formation of a rippled bed (Figure 2b). In contrast, bed motion continued throughout the test duration in Tests 4–6 with higher EPS content, and showing consistent pore pressure (Figure 2d).

3.4. Effect of EPS on Sediment Erosion

Increasing quantities of EPS has a hysteresis effect on the erosion and suspension of sediment. Increasing EPS (Test 2–4) increased the maximum and average SSC level, while further increases of EPS (Test 5 and 6) showed a suppressing effect on erosion, despite of the high mobility of the beds (Table 1 and Figure 2c). The stimulating effect on erosion was particularly apparent in the 0.02% EPS case, where the SSC was highly variable in time and peaked at a value of 19.71 kg/m^3, three times higher than that of the abiotic condition (6.51 kg/m^3) (data shown in Table 1). In lower EPS cases (Test 2 and 3), the decline of SSC correlated with the rapid dissipation of EPP which began at around 800 s (Figure 2b). The increase in SSC was related with the

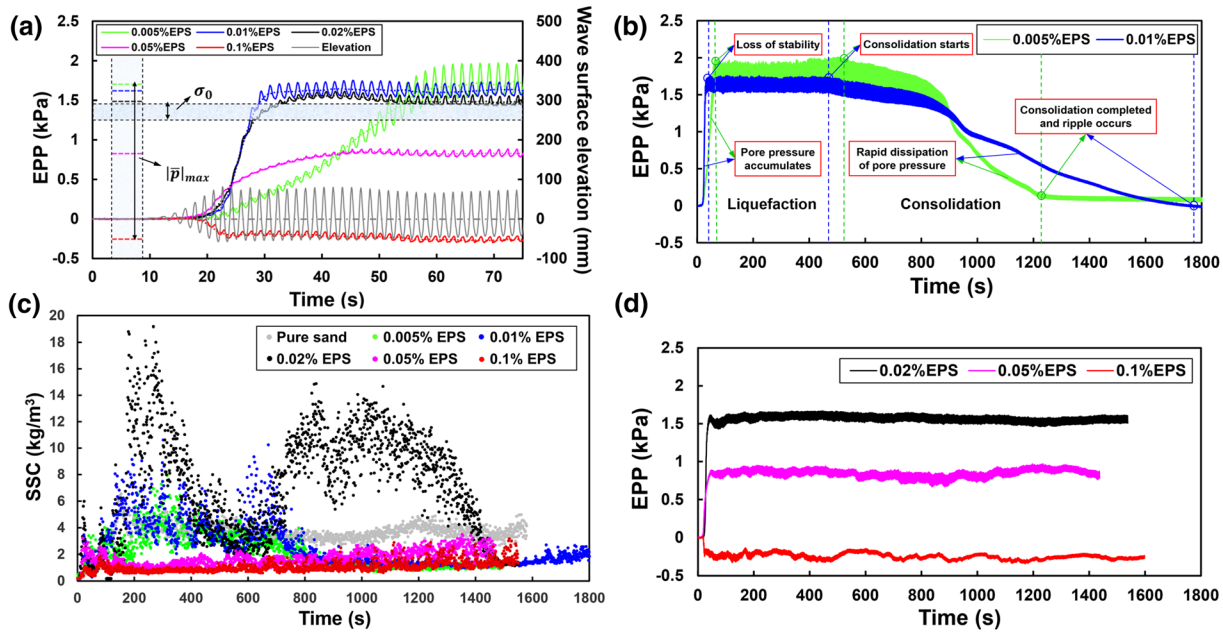

Figure 2. Time series of excess pore water pressure and suspended sediment concentrations. (a) Initial accumulation of pore pressure in beds at a depth of 0.23 cm with different EPS contents. The period-averaged excess-pore pressure (EPP) reaches a constant value $\overline{p}_{\max}$, which is indicated by the dashed horizontal lines in the left-hand column. σ_0 is the initial mean normal effective stress and varied with the addition of EPS within the range indicated. Wave surface elevations were measured above the test area. (b) The complete time-sequences of EPP variation for Test 2–3. Liquefaction occurs when $\overline{p}_{\max}$ is reached, and there is practically no change in the EPP until consolidation/compaction starts (i.e., the sediment grains come into contact). Dissipation of the pore pressure starts after ~8 min, which is accompanied by a consolidation of the bed. After a consolidation period that varies in length depending on the EPS content, the cyclic mass-motion stops and ripples form on the surface. (c) Time development of suspended sediment concentrations (SSC) for the abiotic condition and biological condition. The SSC was measured 0.04 m above the bed. (d) The complete time-sequences of EPP variation for Test 4–6. EPS, extracellular polymeric substances.

accumulation of EPP at bottom (Figure 2a), which caused an upward seepage flow, moving and suspending sand grains (Jia et al., 2014; Tzang & Ou, 2006). With increasing EPS however, the value of $\overline{p}_{\max}$ decreased (Figure 2a), meanwhile, the higher biological cohesion also hindered SSC by changing the mechanism of bed failure from local to nonlocal, involving many linked grains (Vignaga et al., 2013). Nevertheless, these results are quite different from previous ones obtained under steady flow conditions, where the presence of EPS act as a biological stabilizer, inhibiting erosion and decreasing sediment transport (Chen et al., 2017a; Fang et al., 2017).

3.5. Mechanism of Biological Cohesion Induced Mobility of Sediments

Under the wave crest, the wave pressure in excess of the hydrostatic pressure is positive and the bed tends to decrease in volume (Figure 3a and 3b center). In a well-sorted sand, grains stack up through contact and form a relatively stable structure (Figure 3c). Moderate wave force can only cause a finite displacement of the grains, and a relatively small variation of the pore pressure because of the high permeability of the bed. In contrast, biosedimentary beds are made up of an amorphous mixture of grains, organics, organisms and pore spaces, with EPS attaching to available surfaces or bridging between adjacent particles (Figures 3c, 3e–3g) (Chen et al., 2017b; Paterson et al., 2000; Van Colen et al., 2014; N. Zhang et al., 2018). The sand-EPS skeleton is rearranged at the expense of the pore volume, where the EPS bridges break and deform due to shear forces and torques (Figure 3c center). As a result, the waves compresses the sediment particles closer together, producing a plastic deformation as the original internal structure is changed. Such movement reduces the conveyance capacity of the interstices, and impedes the travel of the pressure wave through the sediment. The pore water pressure is therefore increased, which substantially lowers the effective stress of the bed and hence the bed resistance to shear stress.

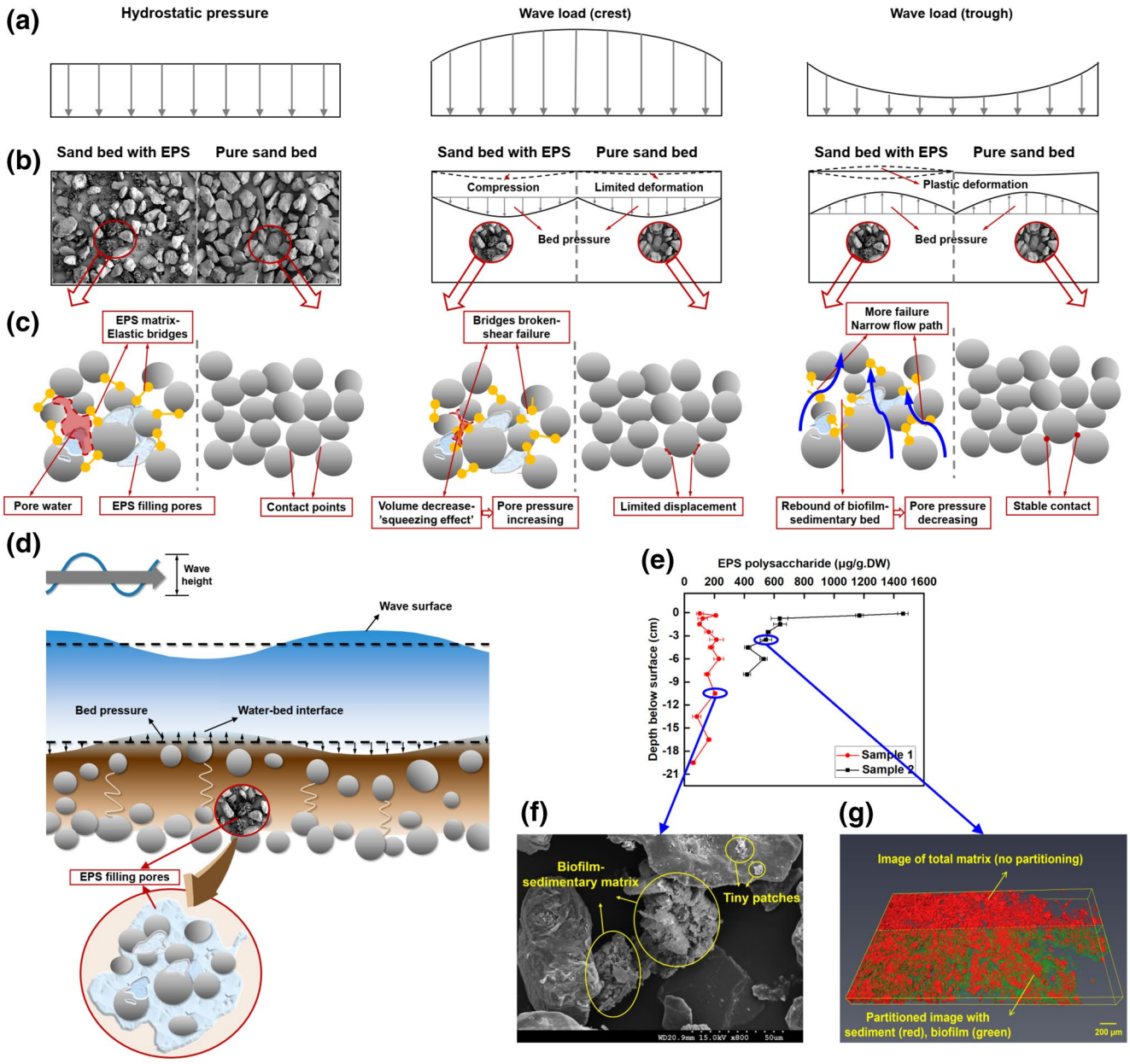

Note: the "compression" or "deformation" of the bed only represents a "tendency" before the liquefaction occurs, after which a fluid-like motion of the bed can be observed, and the sediment-water interface oscillates.

Figure 3. Schematic of mechanism for EPS (low content) induced liquefaction of a sandy bed. Under load from the hydrostatic condition (left column) and wave forcing (crest, center column and trough, right column, respectively) (a), the bed responds differently for the biological condition (left) and abiotic condition (right) (b). The images in (b) are SEM images. The grain-EPS-grain contact and the excess-pore water response are represented at the μm scale (c). In the case with a high EPS content (i.e., 0.1%), a wave induces the composite elastic bed of sediment and EPS into synchronized mechanical oscillation (d). The elastic properties of the bed allow an immediate deformation of the bed, almost synchronous with the periodic pressure variation, whereby the water-bed interface is (nearly) 180° out of phase with the wave surface. Vertical profiles of EPS in flat beds were taken from the bare flat area, Jiangsu Coast, China (Sample 1, the median grain diameter, D_{50}, was 0.105 mm) and the natural salt marsh area, Eden Estuary, UK (Sample 2, D_{50} = 0.180 mm) (e). In bed with lower EPS content of 0.005–0.020% (e, sample 1), aggregates of biofilm and smaller grains are shown, while small patches of biofilm are attached to the surface of larger grains (f, scanning electron microscope image, sample freezing-dried). The biofilm-sedimentary matrixes are of greater integrity with higher EPS content (e, 0.040–0.150%, sample 2), shown by the nondestructive 3D image (sample hydrated) using x-ray microcomputed tomography (g). See supporting information Text S2 and S3 for information about the field sites. Such structures imply that the liquefaction susceptibility of a certain depth layer of natural sediments may be affected by the biological cohesion. EPS, extracellular polymeric substances; SEM, scanning electron microscopy.

Under the wave trough the bed rebounds, and the pore pressure reduces (Figure 3a and 3b, right). Seepage flow induces an upward drag on the grains due to the pressure gradient, passing through the pores where the hydraulic conveyance of the bed is reduced by EPS (Figure 3c, right) (Geng et al., 2017; Volk et al., 2016). EPS bridges would be further destroyed due to the relative displacement. Consequently, this cyclic process of collapse and rebound forces the grains closer together, and compresses the pore water between the particles.

However, for the biological condition with 0.1% EPS, the response of the bed changes significantly. The bed deforms immediately from the onset of wave action without a solid-liquid transition, and behaves in a similar manner to fluid mud, which only fine cohesive sediment can form (Figure 3d, see Figure S5 for the rheological properties of the EPS 0.1%-sand mixture). The grain-grain skeleton is augmented by an EPS skeleton with grains embedded in an EPS matrix (Figure 3g). A Rayleigh-Taylor instability may also arise, where an upward drag force can increase locally due to a buoyancy effect, which causes channeling of EPS (lighter fluid) to push through denser sands (McLaren et al., 2019). Previous studies have shown the formation of volcano-like "water escape structures" (McLaren et al., 2019; Nichols et al., 1994), in which the upwelling pore EPS fluid can be squeezed out from the bottom sand structure, along with gas bubbles (Figure S6), creating a "vacuum effect" for the pore water, which explains the occurrence of negative pore pressure (Figure 2a). It should be noted that in this experiment xanthan gum was used as an EPS proxy to provide biological cohesion, which contains no protein, however the real EPS matrix may be more complex (Figures 3e–3g; Flemming & Wingender, 2010).

4. Implications and Conclusions

The experimental data in this study show that the pervasive distribution of microbial EPS with a mass concentration of 0.005%–0.1% throughout the sediment, can be a key factor in wave liquefaction dynamics. The analysis clarifies how neglecting the presence of even low content of EPS can result in inaccurate prediction of the bed stability. This is clearly important for the design of coastal structures and may also be relevant to the correct interpretation of the aleo environmental conditions of sedimentary successions formed by waves. Through sea-level rise, the risk of bed liquefaction is expected to impact more engineering structures and also poses potential threats to wetlands, where microbial communities occupy habitats such as salt marshes and submerged aquatic vegetation beds, where the production of EPS is much higher. The misinterpretation of the vulnerability of wetlands when exposed to waves could put the existing ecosystems at risk, considering that these ecosystem services are valued at about US$10,000 per hectare (Battin et al., 2008; Kirwan & Megonigal, 2013). These findings also expand the known diversity of behaviors from organic matter that moderate global biogeophysical cycles, and interface with the sediment dynamics that can potentially contribute to other major geological events.

Data Availability Statement

Data and the results presented in this study can be obtained through Mendeley Data online (http://dx.doi.org/10.17632/k74dnxrfcf.1).

Acknowledgments
Funding for this project was provided by the National Key Research and Development Project, MOST, China (2018YFC0407506), the National Natural Science Foundation of China (51620105005), and the China Postdoctoral Science Foundation (2020M680580). D. M. Paterson acknowledges NERC funding (N E/N016009/1). We appreciate the work of Dr. Naiyu Zhang for the nondestructive three dimensional imaging of the biofilm-sediments. We would like to thank Jun Zhang, Fei Gao, Guangwei Liu and Kaiyue Shan for the fruitful discussions. Our thanks also go to Jia Xu, Shibai Yu and all our laboratory assistants for their help with the flume setup.

References

Battin, T. J., Kaplan, L. A., Findlay, S., Hopkinson, C. S., Marti, E., Packman, A. I., et al. (2008). Biophysical controls on organic carbon fluxes in fluvial networks. *Nature Geoscience*, *1*(8), 95–100.

Chen, X. D., Zhang, C. K., Paterson, D. M., Thompson, C. E. L., Townend, I. H., Gong, Z., et al. (2017a). Hindered erosion: The biological mediation of noncohesive sediment behavior. *Water Resources Research*, *53*, 4787–4801. https://doi.org/10.1002/2016WR020105

Chen, X. D., Zhang, C. K., Zhou, Z., Gong, Z., Zhou, J. J., Tao, J. F., et al. (2017b). Stabilizing effects of bacterial biofilms: EPS penetration and redistribution of bed stability down the sediment profile. *Journal of Geophysical Research Biogeosciences*, *122*, 3113–3125. https://doi.org/10.1002/2017JG004050

Chung, S. G., Kim, S. K., Kang, Y. J., Im, J. C., & Nagendra Prasad, K. (2006). Failure of a breakwater founded on a thick normally consolidated clay layer. *Geotechnique*, *56*(6), 393–409.

Craig, M. J., Baas, J. H., Amos, K. J., Strachan, L. J., Manning, A. J., Paterson, D. M., et al. (2020). Biomediation of submarine sediment gravity flow dynamics. *Geology*, *48*, 72–76.

Danovaro, R., Corinaldesi, C., Rastelli, E., & Dell'Anno, A. (2015). Toward a better quantitative assessment of the relevance of deep-sea viruses, Bacteria and Archaea in the functioning of the ocean seafloor. *Aquatic Microbial Ecology*, *75*(1), 81–90.

Davis, C. A., Atekwana, E., Atekwana, E., Slater, L. D., Rossbach, S., & Mormile, M. R. (2006). Microbial growth and biofilm formation in geologic media is detected with complex conductivity measurements. *Geophysical Research Letters*, *33*(18), 122–140.

Fang, H. W., Lai, H. J., Cheng, W., Huang, L., & He, G. J. (2017). Modeling sediment transport with an integrated view of the biofilm effects. *Water Resources Research*, *53*(9), 7536–7557.
Flemming, H., & Wingender, J. (2010). The biofilm matrix. *Nature Reviews Microbiology*, *8*(9), 623–633.
Flemming, H., & Wuertz, S. (2019). Bacteria and archaea on Earth and their abundance in biofilms. *Nature Reviews Microbiology*. *17*, 247–260. https://doi.org/10.1038/s41579-019-0158-9
Franco, L. (1994). Vertical breakwaters: The Italian experience. *Coastal Engineering*, *22*(suppl 1–2), 31–55.
Garcı A-Ochoa, F., Santos, V. E., Casas, J. A., & Gómez, E. (2000). Xanthan gum: Production, recovery, and properties. *Biotechnology Advances*, *18*(7), 549–579.
Geng, X., Heiss, J. W., Michael, H. A., & Boufadel, M. C. (2017). Subsurface flow and moisture dynamics in response to swash motions: Effects of beach hydraulic conductivity and capillarity. *Water Resources Research*, *53*(12), 10317–10335.
Gerbersdorf, S. U., & Wieprecht, S. (2015). Biostabilization of cohesive sediments: revisiting the role of abiotic conditions, physiology and diversity of microbes, polymeric secretion, and biofilm architecture. *Geobiology*, *13*(1), 68–97. https://doi.org/10.1111/gbi.12115
Gratchev, I. B., Sassa, K., Osipov, V. I., & Sokolov, V. N. (2006). The liquefaction of clayey soils under cyclic loading. *Engineering Geology*, *86*(1), 70–84.
Jia, Y. G., Zhang, L. P., Zheng, J. W., Liu, X. L., Jeng, D. S., & Shan, H. X. (2014). Effects of wave-induced seabed liquefaction on sediment re-suspension in the Yellow River Delta. *Ocean Engineering*, *89*, 146–156.
Kirwan, M. L., & Megonigal, J. P. (2013). Tidal wetland stability in the face of human impacts and sea-level rise. *Nature*, *504*(7478), 53–60.
Lambe, T. W., & Whitman, R. V. (1969). *Soil mechanics*. New York: Wiley.
Le Hir, P., Monbet, Y., & Orvain, F. (2007). Sediment erodability in sediment transport modeling: Can we account for biota effects? *Continental Shelf Research*, *27*(8), 1116–1142. https://doi.org/10.1016/j.csr.2005.11.016
Lewis, J. B., & Partridge, B. A. (1967). Fluidization. *Nature*, *216*(5111), 124–127.
Marani, M., D'Alpaos, A., Lanzoni, S., Carniello, L., & Rinaldo, A. (2007). Biologically-controlled multiple equilibria of tidal landforms and the fate of the Venice lagoon. *Geophysical Research Letters*, *34*(11), L11402., doi: https://doi.org/10.1029/2007GL030178
Mariotti, G., Pruss, S. B., Perron, J. T., & Bosak, T. (2014). Microbial shaping of sedimentary wrinkle structures. *Nature Geoscience*, *7*(10), 736–740. https://doi.org/10.1038/NGEO2229
Mcanally, W. H., Friedrichs, C., Hamilton, D., Hayter, E., Shrestha, P., Rodriguez, H., et al. (2007). Management of Fluid Mud in Estuaries, Bays, and Lakes. I: Present state of understanding on character and behavior. *Journal of Hydraulic Engineering*, *133*(1), 9–22.
McLaren, C. P., Kovar, T. M., Penn, A., Müller, C. R., & Boyce, C. M. (2019). Gravitational instabilities in binary granular materials. *Proceedings of the National Academy of Sciences*, *116*(19), 9263–9268.
Mountjoy, J. J., Howarth, J. D., Orpin, A. R., Barnes, P. M., Bowden, D. A., Rowden, A. A., et al. (2018). Earthquakes drive large-scale submarine canyon development and sediment supply to deep-ocean basins. *Science Advances*, *4*, r3748.
Nichols, R. J., Sparks, R. S. J., & Wilson, C. J. N. (1994). Experimental studies of the fluidization of layered sediments and the formation of fluid escape structures. *Sedimentology*, *41*, 233–253.
Noffke, N., Eriksson, K. A., Hazen, R. M., & Simpson, E. L. (2006). A new window into Early Archean life: Microbial mats in Earth's oldest siliciclastic tidal deposits. *Geology*, *34*, 253–256.
Packman, A. (2013). RIVERS building bacterial bridges. *Nature Geoscience*, *6*(9), 682–683. https://doi.org/10.1038/ngeo1938
Parsons, D. R., Schindler, R. J., Hope, J. A., Malarkey, J., Baas, J. H., & Peakall, J. (2016). The role of bio-physical cohesion on subaqueous bedform size. *Geophysical Research Letters*, *43*(4), 1566–1573. https://doi.org/10.1002/2016GL067667
Paterson, D. M. (1989). Short-term changes in the erodibility of intertidal cohesive sediments related to the migratory behavior of epipelic diatoms. *Limnology & Oceanography*, *34*(1), 223–234.
Paterson, D. M., Hope, J. A., Kenworthy, J., Biles, C. L., & Gerbersdorf, S. U. (2018). Form, function and physics: The ecology of biogenic stabilization. *Journal of Soils and Sediments*, *18*(10), 3044–3054.
Paterson, D. M., Tolhurst, T. J., Kelly, J. A., Honeywill, C., de Deckere, E., Huet, V., et al. (2000). Variations in sediment properties, Skeffling mudflat, Humber Estuary, UK. *Continental Shelf Research*, *20*(10–11), 1373–1396. https://doi.org/10.1016/S0278-4343(00)00028-5
Spears, B. M., Saunders, J. E., Davidson, I., & Paterson, D. M. (2008). Microalgal sediment biostabilisation along a salinity gradient in the Eden Estuary, Scotland: Unraveling a paradox. *Marine and Freshwater Research*, *59*(4), 313.
Sumer, B. M. (2009). Liquefaction around marine structures. In *Coastal Structures -Coastal Structures International Conference*. https://www.researchgate.net/deref/http%3A//dx.doi.org/10.1142/9789814282024_0164
Sumer, B. M., Hatipoglu, F., FredsØe, J., & Sumer, S. K. (2006). The sequence of sediment behavior during wave-induced liquefaction. *Sedimentology*, *53*, 611–629.
Sumer, B. M., Kirca, V. S. O., & Fredsøe, J. (2012). Experimental validation of a mathematical model for seabed liquefaction under waves. *International Journal of Offshore and Polar Engineering*, *22*(2), 133–141.
Taylor, I. S., & Paterson, D. M. (1998). Microspatial variation in carbohydrate concentrations with depth in the upper millimetres of intertidal cohesive sediments. *Estuarine, Coastal and Shelf Science*, *46*, 359–370.
Tolhurst, T. J., Gust, G. & Paterson, D. M. (2002). The influence of an extracellular polymeric substance (EPS) on cohesive sediment stability. *Fine Sediment Dynamics in the Marine Environment*, *5*, 409–425.
Travis, J. (2005). Hurricane Katrina: Scientists' fears come true as hurricane floods New Orleans. *Science*, *309*(5741), 1656–1659.
Tzang, S., & Ou, S. (2006). Laboratory flume studies on monochromatic wave-fine sandy bed interactions Part 1. *Soil Fluidization Coastal Engineering*, *53*(11), 965–982.
Van Colen, C., Underwood, G. J. C., Serôdio, J., & Paterson, D. M. (2014). Ecology of intertidal microbial biofilms: Mechanisms, patterns and future research needs. *Journal of Sea Research*, *92*(SI), 2–5. https://doi.org/10.1016/j.seares.2014.07.003
Vignaga, E., Sloan, D. M., Luo, X., Haynes, H., Phoenix, V. R., & Sloan, W. T. (2013). Erosion of biofilm-bound fluvial sediments. *Nature Geoscience*, *6*(9), 770–774. https://doi.org/10.1038/NGEO1891
Volk, E., Iden, S. C., Furman, A., Durner, W., & Rosenzweig, R. (2016). Biofilm effect on soil hydraulic properties: Experimental investigation using soil-grown real biofilm. *Water Resources Research*, *52*, 5813–5828.
Zhang, N., Thompson, C. E. L., Townend, I. H., Rankin, K. E., Paterson, D. M., & Manning, A. J. (2018). Nondestructive 3D imaging and quantification of hydrated biofilm-sediment aggregates using X-ray Microcomputed Tomography. *Environmental Science and Technology*, *52*(22), 13306–13313. https://doi.org/10.1021/acs.est.8b03997
Zhang, X., Liu, X., Gu, D., Zhou, W., Xie, T., & Mo, Y. (1996). Rheological models for xanthan gum. *Journal of Food Engineering*, *27*(2), 203–209.